Characterisation of a Compact Neutron Spectrometer and unfolded neutron emission spectra in ASDEX Upgrade

G. Tardini[1], R. Fischer[1], F. Gagnon-Moisan[2,3], M. Weiland[1], A. Zimbal[2]
and the ASDEX Upgrade Team

[1] Max-Planck-Institut für Plasmaphysik, Boltzmannstr. 2, 85748 Garching, Germany

[2] Physikalisch-Technische Bundesanstalt, Bundesallee 100, 38116 Braunschweig, Germany

[3] Paul Scherrer Institut, 5232 Villigen PSI, Switzerland

1 Introduction

The physics of fast ions is a crucial issue in future burning plasmas like ITER due to their potential damage of first wall components as well as possible confinement deterioration. Fast ion generation and transport have been therefore subject of extensive investigations and diagnostic development in the last decade.

The energy spectrum of fusion neutrons is a footprint of the fast ion distribution, because the kinetic energy of the deuterons affects the energy of the fusion neutron, on top of the energy of 2.452 MeV carried by a neutron from the d-d reaction at rest.

A Compact Neutron Spectrometer (CNS) is installed at the ASDEX Upgrade tokamak [1][2]. It measures Pulse Height Spectra (PHS), resulting from the convolution of the neutron energy spectrum with the instrumental response function. While the PHS can provide evidence for higher energetic tails of the fast ion distribution [3], a quantitative evaluation requires the unfolded Neutron Emission Spectra (NES).

In this paper we discuss the characterisation of the detector and its response function. Moreover, the first unfolded NES are presented. Two phases of the same Neutral Beam Injection (NBI) heated discharge are compared: one with Ion Cyclotron Range of Frequency (ICRF) on top, and one without. A direct measurement of the NES tails and a comparison with Line-Of-Sight (LOS) simulated spectra provide a quantitative evaluation of the fast ion energy distribution.

2 Characterisation of the detector

For a given incoming neutron energy, the CNS detects a full energy spectrum of recoil protons, due to the random scattering angle. The scintillator properties and geometry, as well as the detector efficiency, make this response individual from detector to detector. Therefore, the response of the CNS to neutrons for different known energies has to be determined in order to unfold the experimental PHS.

Such responses were measured at the facility of the Physikalisch-Technische Bundesanstalt (PTB), with a white neutron field in the interval 1-17 MeV. As the distance of the detector to the neutron source is fixed, we can select narrow intervals of the neutron energy via their time-of-flight, and measure the associated PHS. A set of PHS is simulated with the NRESP code [4] for the same energies. Such synthetic PHS are then fitted to the experimental ones, assuming an energy dependent Gaussian broadening and using the maximum entropy of the solution as an optimisation criterium [5]. The results are shown in Fig. 1 .

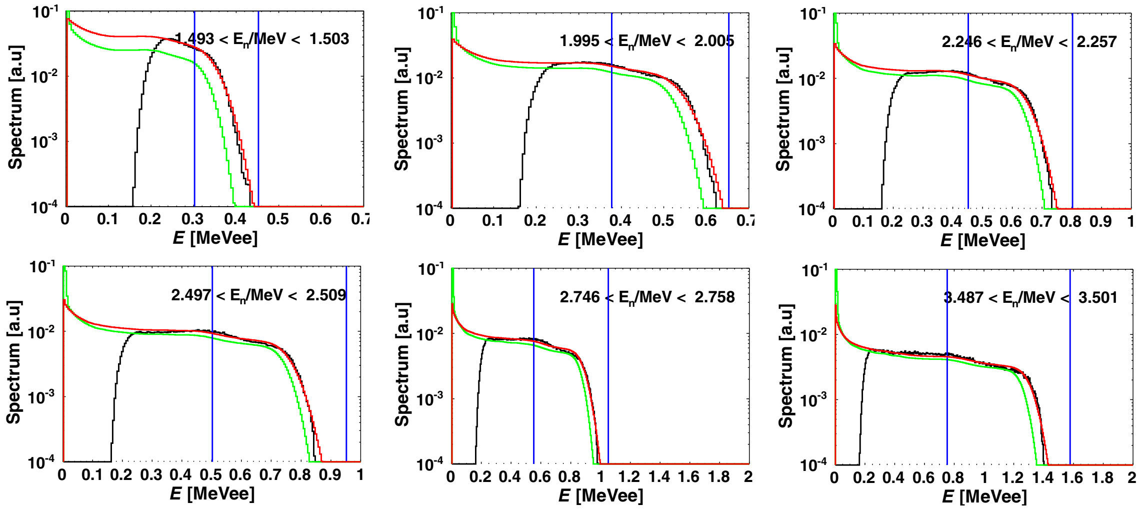

Figure 1 . Detector response at several energies. Measured (black), simulated (green), optimised (red). The blue vertical lines delimit the region used for the fit.

The fit in Fig. 1 matches the experimental results accurately over several orders of magnitude, while the statistical noise of the measurements is avoided. This is needed for accurate unfolding, so the fitted response matrix is the one used for deconvolution purposes.

The response for selected energy intervals is compared to that of monoenergetic neutrons, generated with the cyclotron of the PTB facility. A deuterium beam is accelerated towards a deuterium gas target, while the detector measures the neutrons from the D-d fusion. The comparison is shown in Fig. 2 .

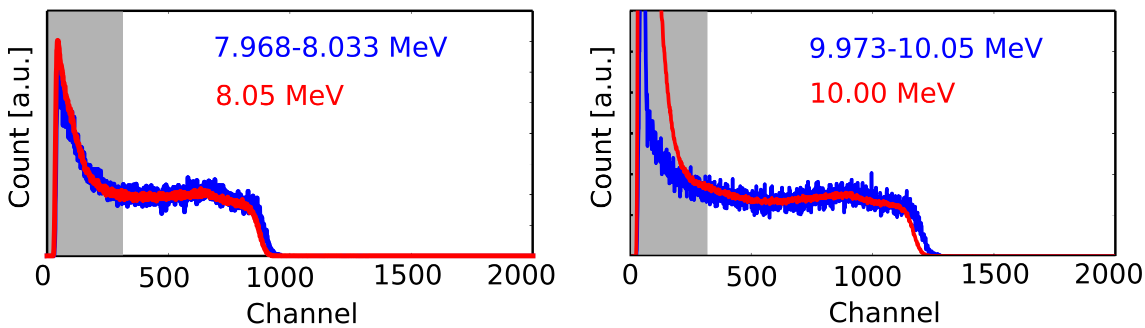

Figure 2 . Detector response at E_n=8 and 10 MeV. Selecting energy interval from time-of-flight measurement (blue), monoenergetic (red).

The shapes of the responses for 8 and 10 MeV in Fig. 2 agree well with the time-of-flight PHS concerning the slope, while the position of the edge is slightly lower for the monoenergetic neutrons. For low channels, the PHS of monoenergetic neutrons is dominated by other reactions and it should not be considered for the comparison.

3 Detection of ICRF 2nd harmonic D-acceleration

Two different PHS have been measured for the H-mode discharge # 29795 in a phase with NBI heating only and a later phase where ICRF was added (see [3]). Now the detector's response function is used to unfold both measured PHS, using a method based on maximum entropy [6]. The outcome is displayed in Fig. 3 (a).

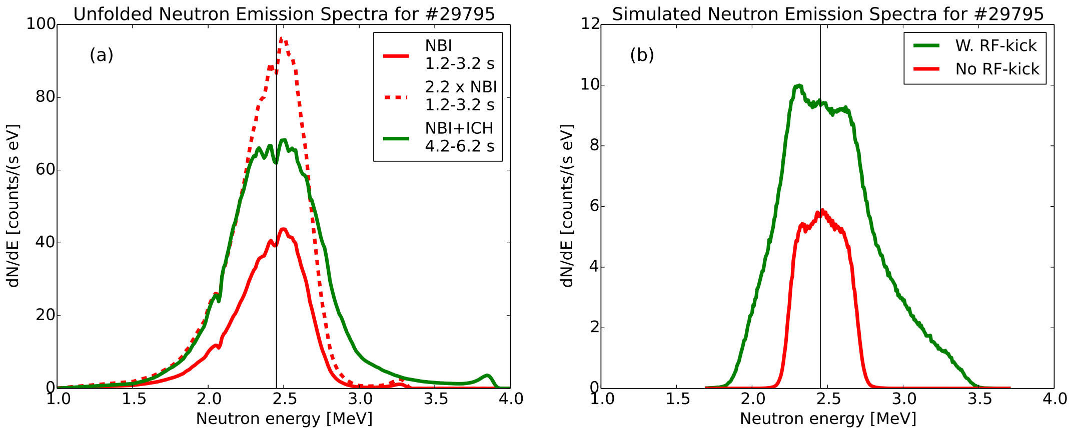

Figure 3 . NES of discharge # 29795 (a) Unfolding the measured PHS. NBI-only (continous red), NBI-only multiplied by 2.2 for shape comparison (red dashed), NBI+ICRF (green). (b) LoS simulation: without (red) and with the RF-kick operator (green).

The strong energetic tail in case of NBI+ICRF is clearly visible in Fig. 3 (a), as the green curve extends way beyond the red dashed (NES of the NBI-only phase multiplied by an ad-hoc factor). The maximum energy of the fast ions can be estimated by looking at the maximum ΔE_n with respect to the reference value of 2.452 MeV (black vertical line). In fact, from simple kinematic considerations one has $\Delta E_n \approx \sqrt{E_{fus} E_{f.i.max}}$, where $E_{fus} =$ 2.452 MeV is the reference d-d neutron energy and $E_{f.i.max}$ the maximum fast ion energy in the considered plasma. Substituting $E_{f.i.max} = 60$ keV (the NBI energy applied in this discharge) one obtains $\Delta E_n \approx 0.4$ MeV, which is observed for the red curve of Fig. 3 (a). A $\Delta E_n = 1$ MeV, exhibited by the green curve in Fig. 3 (a) corresponds to $E_{f.i.max} \approx$ 400 keV.

The effect of the synergy between ICRF and NBI can be simulated [11][3], in particular in the TRANSP code [8] since a RF-kick operator was implemented [9]. In Fig. 4 the NBI+ICRF is simulated with and without RF-kick operator, while keeping the same background plasma as simulation input.

When the RF-kick operator is included, fast deuterons are accelerated up to ~ 500 keV (see Fig. 4 (b)). The resulting distribution function is used as input in the GENESIS code [10], which calculates the NES in the proper LOS of the detector. The code prediction for both cases is shown in Fig. 3 (b), with the same colour code. There is a qualitative agreement with the experimental unfolded NES in Fig. 3 (a). However, it appears that the high energy tail of the neutron distribution is overestimated, while the low energy end the tail is less pronounced.

4 Conclusions

The CNS installed at ASDEX Upgrade is now fully characterised. The response matrix is obtained by fitting simulated PHS to the measured response at given neutron energies, selected by the neutron time-of-flight. This is accurate and smooth enough to unfold the experimental PHS [5].

The first examples of unfolded NES for ASDEX Upgrade are presented and discussed

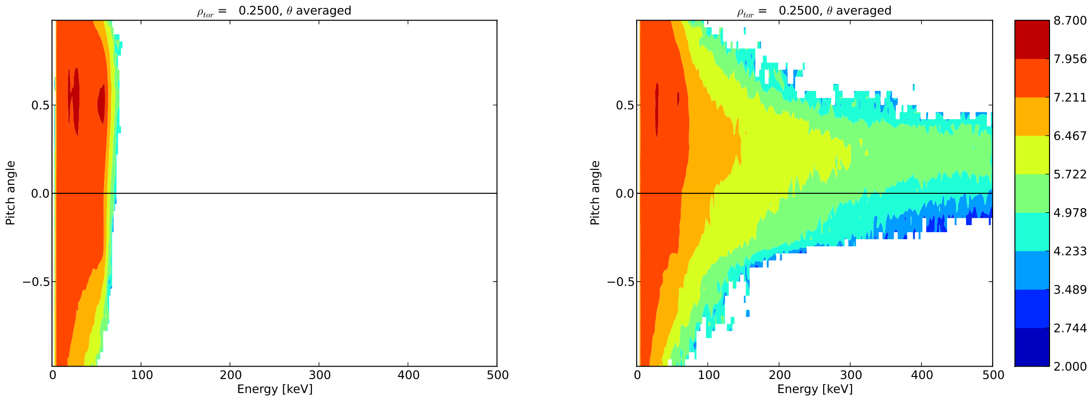

Figure 4 . Logarithmic TRANSP fast ions distribution functions as a function of energy and pitch angle at $\rho_{tor} = 0.25$. D with higher energy is predicted in presence of ICRF (right plot).

here, providing clear evidence of fast deuterium acceleration by direct ICRF 2nd harmonic heating. An upper limit of the fast ions present in the tokamak can be derived directly from the unfolded spectrum, amounting roughly to 1 MeV. The experimental NES can be compared to the LOS prediction obtained coupling the fast-ions orbit following code TRANSP and the GENESIS code, calculating fusion reactions along a LOS. The prediction is qualitatively good and the enhancement due to the RF-kick is in quantitative agreement with the unfolded experimental NES. The simulated neutron spectrum has a a slightly different shape, with a stronger tail at the high energy end but less pronounced at the low energy end. A comparison with the prediction of the TORIC6 code, coupled to a Fokker-Planck solver [11], is underway.

Weight functions of the diagnostic have been calculated, in order to combine several fast ions diagnostics in overlapping regions of the veocity space.

References

[1] G. Tardini *et al.*, Journal of Instrumentation **7** (2012) C03004

[2] L. Giacomelli *et al.*, Review of Scientific Instrument **82** (2011) 123504

[3] G. Tardini *et al.*, 41th EPS Conference on Plasma Physics, O2.103 (2014)

[4] G. Dietzke and H. Klein, Physikalisch-Technische Bundesanstalt Report PTB-ND-22, Braunschweig, Germany (1982), ISSN 0572-7170

[5] F. Gagnon-Moisan *et al.*, Journal of Instrumentation **7** (2012) C02023

[6] M. Reginatto, A. Zimbal, Rev. Sci. Instruments **79** (2008) 023505 [11] R. Bilato *et al.*, Nuclear Fusion **51** (2011) 103034

[8] A. Pankin, D. McCune, R. Andre *et al*, Comp. Phys. Comm. **159**, No. 3 (2004) 157

[9] B. H. Park *et al.*, Paper JP8.00122, Bull. Am. Phys. Soc. 54, (2012)

[10] M. Nocente *et al.*, Nuclear Fusion **51** (2011) 063011

[11] R. Bilato *et al.*, Nuclear Fusion **51** (2011) 103034

Acknowlegment: This work has been carried out within the framework of the EUROfusion Consortium and has received funding from the Euratom research and training programme 2014-2018 under grant agreement No 633053. The views and opinions expressed herein do not necessarily reflect those of the European Commission.